



## Upconversion luminescence in $\text{Er}^{3+}/\text{Yb}^{3+}$ codoped $\text{Y}_2\text{CaGe}_4\text{O}_{12}$

I.I. Leonidov<sup>a,\*</sup>, V.G. Zubkov<sup>a</sup>, A.P. Tyutyunnik<sup>a</sup>, N.V. Tarakina<sup>a</sup>, L.L. Surat<sup>a</sup>, O.V. Koryakova<sup>b</sup>, E.G. Vovkotrub<sup>c</sup>

<sup>a</sup> Institute of Solid State Chemistry, Ural Branch of RAS, 620990 Ekaterinburg, Russia

<sup>b</sup> I.Ya. Postovsky Institute of Organic Synthesis, Ural Branch of RAS, 620990 Ekaterinburg, Russia

<sup>c</sup> Institute of High-Temperature Electrochemistry, Ural Branch of RAS, 620219 Ekaterinburg, Russia

### ARTICLE INFO

#### Article history:

Received 3 August 2010

Received in revised form 1 October 2010

Accepted 10 October 2010

Available online 21 October 2010

#### Keywords:

Upconversion

Luminescence

Ceramics

Oxide materials

Optical properties

Raman spectroscopy

### ABSTRACT

Calcium yttrium tetrametagermanates  $\text{Y}_2\text{CaGe}_4\text{O}_{12}$  doped with  $\text{Er}^{3+}$  and  $\text{Er}^{3+}/\text{Yb}^{3+}$  reveal upconversion emission in visible spectral range under near-infrared excitation,  $\lambda_{\text{ex}} = 980 \text{ nm}$ . For the solid solution  $\text{Er}_x\text{Y}_{2-x}\text{CaGe}_4\text{O}_{12}$  concentration dependencies for the green and red lines of the visible emission around  $526 \text{ nm}$  ( ${}^2\text{H}_{11/2} \rightarrow {}^4\text{I}_{15/2}$ ),  $545 \text{ nm}$  ( ${}^4\text{S}_{3/2} \rightarrow {}^4\text{I}_{15/2}$ ) and  $670 \text{ nm}$  ( ${}^4\text{F}_{9/2} \rightarrow {}^4\text{I}_{15/2}$ ) show the optimal value for the sample  $x = 0.2$ . The power dependence of the visible luminescence measured at room temperature in the low-power limit indicates two-photon upconversion process. Direct intensification of the upconversion emission signals has been achieved by ytterbium sensitizing. The other upconversion excitation mechanism in  $\text{Y}_2\text{CaGe}_4\text{O}_{12}:\text{Er}^{3+}$  is discussed for an  $808 \text{ nm}$  incident laser irradiation. A scheme of excitation and emission routes involving ground/excited state absorption, energy transfer upconversion, nonradiative multiphonon relaxation processes in trivalent lanthanide ions in  $\text{Y}_2\text{CaGe}_4\text{O}_{12}:\text{Er}^{3+}$  and  $\text{Y}_2\text{CaGe}_4\text{O}_{12}:\text{Er}^{3+}, \text{Yb}^{3+}$  has been proposed. Conditions for visible emission occurrence under quasi-resonance  $\lambda_{\text{ex}} = 1064 \text{ nm}$  excitation depending on pump power values are considered. In the low-power regime only near-infrared emission caused by the transition  ${}^4\text{I}_{13/2} \rightarrow {}^4\text{I}_{15/2}$  in erbium ions has been detected.

© 2010 Elsevier B.V. All rights reserved.

### 1. Introduction

In the last few decades much attention has been paid to the research on rare-earth doped upconversion luminescent materials owing to their application in various technological fields, such as high power diodes engineering, coherent laser sources [1], three-dimensional displays [2,3], and bioassays [4]. Realization of solid state RGB light emitters as the basis for future high brightness full-color display technology requires the generation and intensity control of the three fundamental red, green, and blue (RGB) light colors in bulk materials. Among various sources for resulting luminescence in visible region there are simultaneous three primary color laser systems based on dye mixtures [5], LED/OLED technologies [6], upconversion of infrared (IR) irradiation [7]. The generation of visible radiation through infrared-to-visible upconversion in lanthanide doped materials has been extensively investigated in the past decades. There are various crystal matrices doped with lanthanide ions ( $\text{Er}^{3+}$ ,  $\text{Yb}^{3+}$ ,  $\text{Tm}^{3+}$ , etc.) in which infrared-to-visible upconversion effect can be observed—chlorides,

fluorides, bromides, oxides. Most of the studies have been performed on single crystals, powders, glasses or glass ceramics. Some kinds of hosts possess low-phonon energy, that results in high upconversion efficiency, e.g.  $\text{KPb}_2\text{Br}_5$  has the maximum phonon energy  $\sim 138 \text{ cm}^{-1}$  [8],  $\text{KPb}_2\text{Cl}_5$  features  $\hbar\omega_{\text{max}} \sim 203 \text{ cm}^{-1}$  [9], oxyfluoride glass ceramics are defined  $\hbar\omega_{\text{max}} \sim 250 \text{ cm}^{-1}$  [10]. Oxide matrices are still investigated widely in the field of optics, and luminescence properties in particular. Crystalline materials with cyclic anions  $[\text{A}_4\text{O}_{12}]$ ,  $\text{A} = \text{P}$  [11,12],  $\text{Si}$  [13],  $\text{V}$  [14],  $\text{Ge}$  [15,16], in the structure are among them. Besides the problem of energy transfer  $\text{Yb}^{3+} \rightarrow \text{Er}^{3+}$  (and/or  $\text{Ho}^{3+}$ ,  $\text{Tm}^{3+}$ ) efficiency the other one lies in effective cooperative energy transfer in the nonresonant systems that may occur via phonon-assisted anti-Stokes sideband excitation [17]. One of the ways to effect the emission, caused by lower excitation energy, is the use of multiphonon-assisted processes originating from inelastic scattering on vibrations in a host matrix. This effect has been found in many rare-earth doped systems [18 and references therein]. Internal vibrations in multicenter cyclic anions  $[\text{Ge}_4\text{O}_{12}]^{8-}$  featuring a group of the new promising optical materials  $\text{Y}_2\text{CaGe}_4\text{O}_{12}$  doped with lanthanide ions can be considered in the case of quasi-resonance energy transfer via phonon-assisted processes.

The above mentioned cyclic structure of anions  $[\text{Ge}_4\text{O}_{12}]^{8-}$  was revealed in a group of tetrametagermanates  $\text{Ln}_2\text{M}^{2+}\text{Ge}_4\text{O}_{12}$ ,  $\text{Ln} = \text{lanthanide or Y}$ ,  $\text{M}^{2+} = \text{Cu}$  [19],  $\text{Ca}$  [20],  $\text{Mn}$  [21],  $\text{Zn}$  [22]. Pow-

\* Corresponding author at: Institute of Solid State Chemistry, Ural Branch of Russian Academy of Sciences, 91, Pervomaiskaya str., GSP, 620990 Ekaterinburg, Russia. Tel.: +7 343 3623521; fax: +7 343 3744495.

E-mail address: [ivanleonidov@ihim.uran.ru](mailto:ivanleonidov@ihim.uran.ru) (I.I. Leonidov).

der samples  $\text{Ln}_2\text{CuGe}_4\text{O}_{12}$ ,  $\text{Ln} = \text{Eu-Lu}$  or  $\text{Y}$ , were first synthesized and described by Lambert and Eysel [23]. The detailed study of crystal and magnetic structures of copper tetrametagermanates stabilized only by  $\text{Ln}^{3+}$  cations smaller than  $\text{Eu}^{3+}$  (S.G.  $P\bar{1}$ ,  $Z=1$ ) was previously discussed [19,24,25]. Specific IR vibrational and Raman spectroscopic features, e.g. in-phase vibrations inside the cycle which result in the appearance of collective vibration modes, have been also reported in Ref. [26]. The strongest Raman lines in the  $100\text{--}1000\text{ cm}^{-1}$  range are attributed to the totally symmetric vibrations. These modes are observed at  $800\text{--}860\text{ cm}^{-1}$  for terminal Ge–O bonds and at  $500\text{--}550\text{ cm}^{-1}$  for the ring (breathing mode). Recently synthesized compounds of the new group of calcium tetrametagermanates  $\text{Ln}_2\text{CaGe}_4\text{O}_{12}$ ,  $\text{Ln} = \text{Y, Eu, Gd, Dy-Lu}$ , crystallize in S.G.  $P4/nbm$ ,  $Z=2$ , keeping the similar cycles in the structure. Layers of discrete  $[\text{Ge}_4\text{O}_{12}]^{8-}$  cycles alternate with layers of metal ions ( $1/2\text{Ca} + 1/2\text{Ln}$ ) in distorted octahedral coordination, and lanthanide ions are in square antiprism coordination [22].

Host matrix  $\text{Y}_2\text{CaGe}_4\text{O}_{12}$  has an optical gap  $\Delta E \sim 4.95(5)\text{ eV}$ . Intense fluorescence in  $\text{Ln}_2\text{CaGe}_4\text{O}_{12}$ ,  $\text{Ln} = \text{Dy}^{3+}, \text{Ho}^{3+}, \text{Er}^{3+}$  and  $\text{Tm}^{3+}$ , caused by  $f\text{--}f$  transitions in rare-earth ions has been found under a  $976\text{ nm}$  laser excitation in the IR range [16]. The full profile structure refinement procedure reveals that erbium ions occupy both eight- and six-coordinated sites in  $\text{Er}_x\text{Y}_{2-x}\text{CaGe}_4\text{O}_{12}$ , but mainly the  $2b$  site with antiprismatic configuration and less the octahedral  $4f$  site with an average ratio of  $0.7/0.3$ . There are two emission centers with different site occupancies in the lattice of  $\text{Er}^{3+}$  doped  $\text{Y}_2\text{CaGe}_4\text{O}_{12}$ . The highest IR emission intensity was recorded for the sample  $x=0.2$ , with only 1% concentration of  $\text{Er}^{3+}$  ions in the lattice ( $7.9 \times 10^{21}$  atoms/ $\text{cm}^3$ ). Although crystal structure properties of  $\text{Ln}_2\text{CaGe}_4\text{O}_{12}$  have been investigated the optical properties of  $\text{Er}^{3+}$  doped and  $\text{Er}^{3+}/\text{Yb}^{3+}$  codoped crystalline yttrium calcium tetrametagermanates have not been studied yet. In this paper, we report luminescence properties of  $\text{Y}_2\text{CaGe}_4\text{O}_{12}:\text{Er}^{3+}$  and  $\text{Y}_2\text{CaGe}_4\text{O}_{12}:\text{Er}^{3+}, \text{Yb}^{3+}$  powders, the possible upconversion emission mechanisms are also discussed.

## 2. Experimental details

$\text{Y}_2\text{CaGe}_4\text{O}_{12}$ ,  $\text{Er}_2\text{CaGe}_4\text{O}_{12}$  and  $\text{Yb}_2\text{CaGe}_4\text{O}_{12}$  powder samples were synthesized by the traditional high-temperature solid state reaction as described elsewhere [20,22], the starting materials were  $\text{Ln}_2\text{O}_3$ ,  $\text{Ln} = \text{Er, Yb, Y}$  (99.99%),  $\text{CaCO}_3$  (99.9%), and  $\text{GeO}_2$  (99.99%). The quality of erbium and ytterbium oxides was proved by optical absorption spectra in visible and near-infrared (NIR) range. As a commercial  $\text{Y}_2\text{O}_3$  might have contained traces of erbium, the yttrium oxide has been annealed at  $1200^\circ\text{C}$  in air, and then possible IR emission, caused by the  $f\text{--}f$  transition

$^4\text{I}_{13/2} \rightarrow ^4\text{I}_{15/2}$  at  $\sim 1550\text{ nm}$  and upconversion emission  $^4\text{S}_{3/2} \rightarrow ^4\text{I}_{15/2}$  at  $545\text{--}552\text{ nm}$  have been checked using a  $980\text{ nm}$  diode laser irradiation. No those emission lines were observed, and spectral intensity did not exceed the standard deviation of the background level when laser power varied up to  $800\text{ mW}$ . Stoichiometric mixtures of initial oxides were pressed into pellets and then placed in alumina crucibles with a lid. Besides  $\text{Y}_2\text{CaGe}_4\text{O}_{12}$ ,  $\text{Er}_2\text{CaGe}_4\text{O}_{12}$  and  $\text{Yb}_2\text{CaGe}_4\text{O}_{12}$  compounds the solid solutions  $\text{Er}_x\text{Y}_{2-x}\text{CaGe}_4\text{O}_{12}$  and  $\text{Er}_x\text{Yb}_y\text{Y}_{2-x-y}\text{CaGe}_4\text{O}_{12}$  have been prepared in microwave furnace at  $1060\text{--}1100^\circ\text{C}$ .

The purity of synthesized products was checked using X-ray powder diffraction patterns collected at room temperature on a STADI P (Stoe) diffractometer in transmission geometry with a linear mini-PSD detector, using  $\text{CuK}\alpha_1$  radiation in the  $2\theta$  range  $2\text{--}120^\circ$  with a step of  $0.02^\circ$ . Polycrystalline silicon ( $a=5.43075(5)\text{ \AA}$ ) was used as external standard. The possible impurity phases were checked by comparing their XRD patterns with those in the PDF2 database (ICDD, USA, Release 2009).

The diffuse reflectance spectra were measured with a Shimadzu UV-2401 PC UV-VIS spectrophotometer using  $\text{BaSO}_4$  as a reference. The photoluminescence (PL) and photoluminescence excitation (PLE) spectra were recorded on a Varian Cary Eclipse fluorescence spectrophotometer coupled to a personal computer with Varian software, and supplied with a  $75\text{ kW}$  Xenon lamp as excitation source (pulse length =  $2\text{ }\mu\text{s}$ , pulse frequency  $\nu=80\text{ Hz}$ , wavelength resolution  $0.5\text{ nm}$ ; PMT Hamamatsu R928). Two diode lasers and one DPSS laser were used as external irradiation sources with excitation wavelengths  $808\text{ nm}$ ,  $980\text{ nm}$ , and  $1064\text{ nm}$  (KLM-H808-120-5, KLM-H980-120-5 manufactured by FTI-Optronic JSC and DMH1064-100 produced by Lsystems Ltd., respectively). Laser power was controlled by a Melles Griot integrated 2-W broadband power/energy meter system BPEM 001. Raman measurements were performed on a Renishaw U1000 spectrometer equipped with a notch filter and CCD detector. Excitation of the samples was provided by the  $514.5\text{ nm}$  radiation from an argon laser. Above listed optical measurements were performed at room temperature. Additional infrared emission spectra in the temperature range  $-180$  to  $200^\circ\text{C}$  were obtained using a Bruker FT-IR spectrometer Vertex 80 combined with a RAMII FT-Raman module (Nd:YAG laser,  $\lambda_{\text{ex}}=1064\text{ nm}$ , Ge detector refrigerated by liquid nitrogen). Infrared absorption spectra were recorded at  $-180^\circ\text{C}$  using the same Bruker FT-IR spectrometer equipped with a liquid nitrogen-cooled InSb detector in the range  $4000\text{--}11,500\text{ cm}^{-1}$ .

## 3. Results and discussion

### 3.1. Upconversion luminescence under 980 nm excitation

Fig. 1 shows the upconversion emission spectra of the  $\text{Y}_2\text{CaGe}_4\text{O}_{12}:\text{Er}^{3+}$  samples under NIR excitation,  $\lambda_{\text{ex}}=980\text{ nm}$ . The strongest emission signal is attained in the solid solution  $\text{Er}_x\text{Y}_{2-x}\text{CaGe}_4\text{O}_{12}$ , where  $x=0.2$ , with 1% content of erbium ions in the lattice ( $7.9 \times 10^{21}$  atoms/ $\text{cm}^3$ ). Concentration dependencies for the lines around  $526\text{ nm}$ ,  $545\text{ nm}$  and  $670\text{ nm}$  are also given in the insets (Fig. 1). Note the compound  $\text{Er}_{0.2}\text{Y}_{1.8}\text{CaGe}_4\text{O}_{12}$  will be designated as  $\text{Y}_2\text{CaGe}_4\text{O}_{12}:\text{Er}^{3+}$  below. For the interpretation of a short-wavelength luminescence, it is often assumed that the order of the upconversion process is the number  $n$  of pump photons

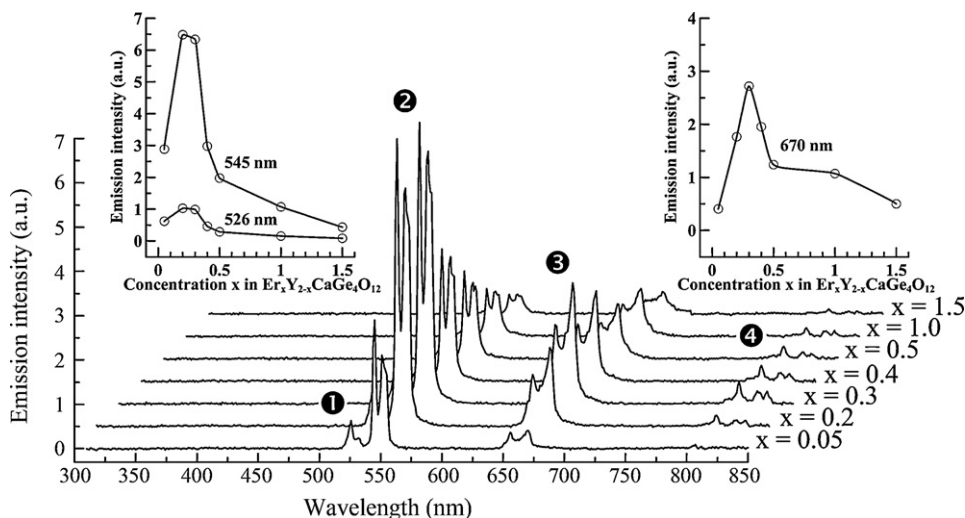


**Fig. 1.** Upconversion emission spectra of the samples  $\text{Er}_x\text{Y}_{2-x}\text{CaGe}_4\text{O}_{12}$ ,  $x=0.05\text{--}1.5$ . The numeration of the bands corresponds to transitions: (1)  $^2\text{H}_{11/2} \rightarrow ^4\text{I}_{15/2}$  ( $526\text{ nm}$ ); (2)  $^4\text{S}_{3/2} \rightarrow ^4\text{I}_{15/2}$  ( $545\text{ nm}$ ); (3)  $^4\text{F}_{9/2} \rightarrow ^4\text{I}_{15/2}$  ( $670\text{ nm}$ ); (4)  $^4\text{I}_{9/2} \rightarrow ^4\text{I}_{15/2}$  ( $806\text{ nm}$ ). In the right inset the concentration dependence is shown for two green lines, in the left one it is given for the red emission. The laser excitation wavelength is  $980\text{ nm}$ .

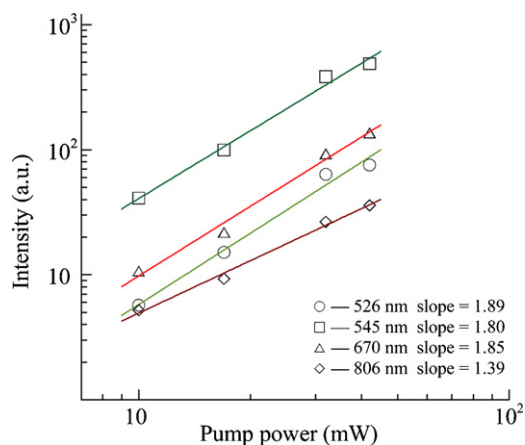


**Fig. 2.** Power dependence of the upconversion luminescence intensity for the  $\text{Er}_{0.2}\text{Y}_{1.8}\text{CaGe}_4\text{O}_{12}$  sample in the low-power regime. The laser excitation wavelength is 980 nm.

required to excite the emitting state. It is indicated by the slope in the graph of the luminescence intensity ( $I$ ) dependence upon the pump power ( $P$ ) in double-logarithmic representation, that is,  $I(P) \propto P^n$ , where  $n$  is the number of NIR photons absorbed to excite one upconversion photon [27].

The power dependence of the three upconversion emissions in visible spectral range is shown in Fig. 2 for the optimized sample  $\text{Er}_{0.2}\text{Y}_{1.8}\text{CaGe}_4\text{O}_{12}$ . Note the spectra have been measured at room temperature in the low-power limit, as a decrease of the slopes takes place at higher powers; that is attributed to the change on the main depopulation mechanism of the excited states [28]. Values of  $n$  obtained for the corresponding 526, 545 and 670 nm emission bands indicate the well-known two-photon upconversion process [29,30].

There is a two-stage process in which the excitation of the  $^4\text{I}_{11/2}$  state resulting from absorption of incident NIR irradiation ( $^4\text{I}_{15/2} \rightarrow ^4\text{I}_{11/2}$ , ground state absorption, or GSA) is followed by a second step consisting on an intra-ion excited state absorption (ESA) and/or inter-ion energy transfer upconversion (ETU). According to the energy level scheme for  $\text{Er}^{3+}$  ions ESA process at 980 nm

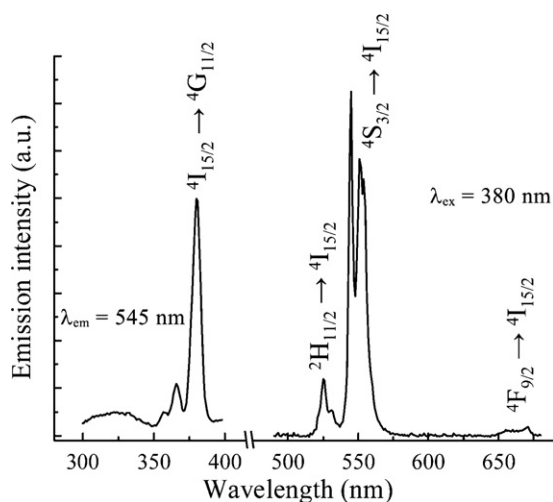


**Fig. 4.** The room temperature emission ( $\lambda_{\text{ex}} = 380 \text{ nm}$ ) and excitation ( $\lambda_{\text{em}} = 545 \text{ nm}$ ) spectra of  $\text{Y}_2\text{CaGe}_4\text{O}_{12}:\text{Er}^{3+}$ .

involves the  $^4\text{I}_{11/2} \rightarrow ^4\text{F}_{7/2}$  transition. The second step of the upconversion may also involve ETU process.

Direct intensification of the visible emission signals due to the corresponding  $f-f$  transitions in  $\text{Er}^{3+}$  ions  $^2\text{H}_{11/2} \rightarrow ^4\text{I}_{15/2}$  ( $\lambda_{\text{em}} = 526 \text{ nm}$ ),  $^4\text{S}_{3/2} \rightarrow ^4\text{I}_{15/2}$  ( $\lambda_{\text{em}} = 545 \text{ nm}$ ),  $^4\text{F}_{9/2} \rightarrow ^4\text{I}_{15/2}$  ( $\lambda_{\text{em}} = 670 \text{ nm}$ ) has been achieved by codoping tetrametagermanate host matrix  $\text{Y}_2\text{CaGe}_4\text{O}_{12}$  with erbium and ytterbium ions (Fig. 3). The synthesis of the solid solution  $\text{Er}_x\text{Yb}_{0.2-x}\text{Y}_{1.8}\text{CaGe}_4\text{O}_{12}$ ,  $x = 0.05\text{--}0.15$ , has been carried out, the optimal value  $x = 0.1$  has been defined. Note the composition  $\text{Er}_{0.1}\text{Yb}_{0.1}\text{Y}_{1.8}\text{CaGe}_4\text{O}_{12}$  is designated as  $\text{Y}_2\text{CaGe}_4\text{O}_{12}:\text{Er}^{3+}, \text{Yb}^{3+}$  to the end of this section. Ytterbium sensitizing and entailing ETU  $\text{Yb}^{3+} \rightarrow \text{Er}^{3+}$  leads to green and red emissions' increasing several times more as it is shown in the inset of Fig. 3. One should note that before mentioned visible emission bands can be registered using a Xe lamp UV excitation, e.g. at 380 nm wavelength, that implies the  $^4\text{I}_{15/2} \rightarrow ^4\text{G}_{11/2}$  transition (Fig. 4). Then the emission from lower energy levels occurs due to nonradiative relaxation from the  $^4\text{G}_{11/2}$  state.

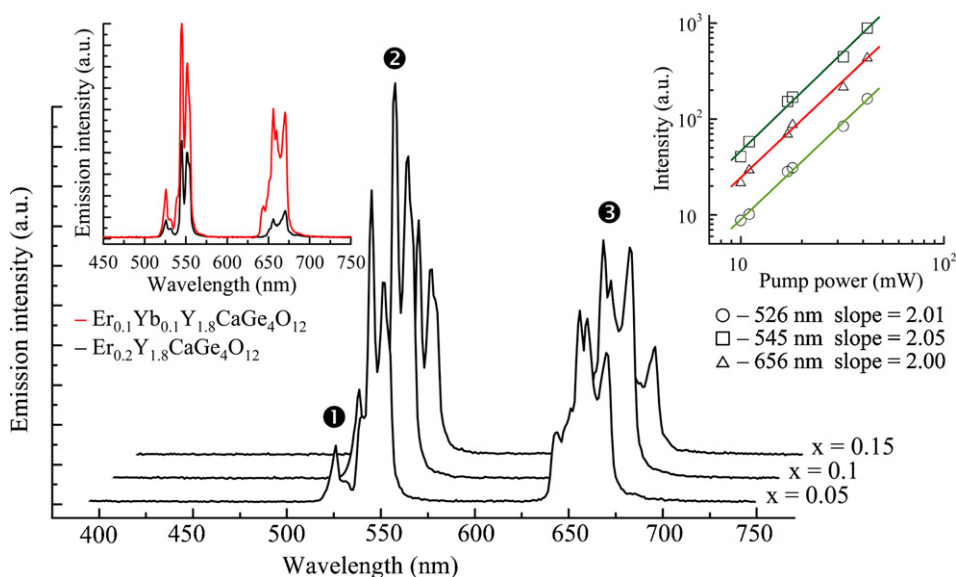


**Fig. 3.** Upconversion emission spectra of the samples  $\text{Er}_x\text{Yb}_{0.2-x}\text{Y}_{1.8}\text{CaGe}_4\text{O}_{12}$ ,  $x = 0.05\text{--}0.15$ . The numeration of the bands corresponds to transitions: (1)  $^2\text{H}_{11/2} \rightarrow ^4\text{I}_{15/2}$  (526 nm); (2)  $^4\text{S}_{3/2} \rightarrow ^4\text{I}_{15/2}$  (545 nm); (3)  $^4\text{F}_{9/2} \rightarrow ^4\text{I}_{15/2}$  (656 nm). The left inset plot shows the intensity comparison for  $\text{Y}_2\text{CaGe}_4\text{O}_{12}:\text{Er}^{3+}, \text{Yb}^{3+}$  and  $\text{Y}_2\text{CaGe}_4\text{O}_{12}:\text{Er}^{3+}$  samples. In the right insertion: power dependence of the upconversion luminescence intensity for the  $\text{Er}_{0.1}\text{Yb}_{0.1}\text{Y}_{1.8}\text{CaGe}_4\text{O}_{12}$  sample in the low-power regime. The laser excitation wavelength is 980 nm.

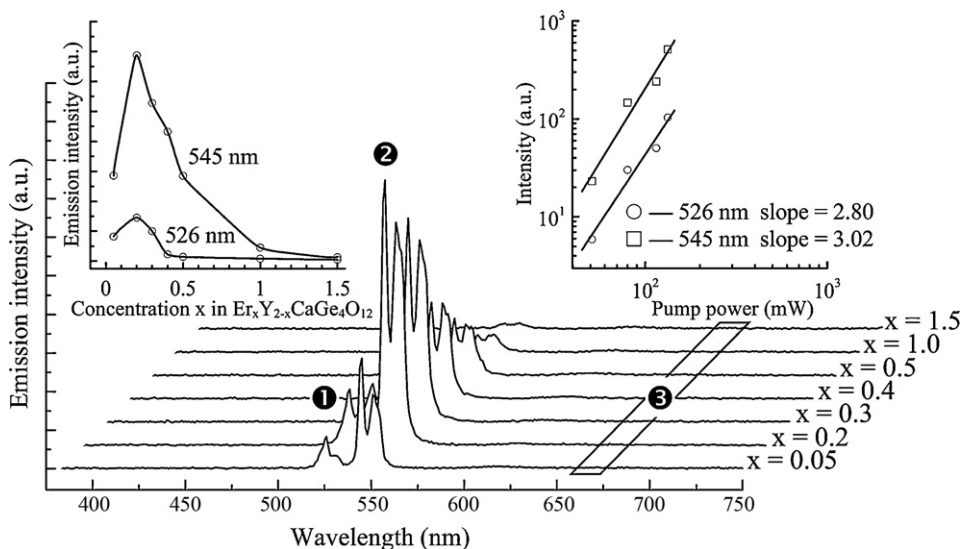


**Fig. 5.** Upconversion emission spectra of the samples  $\text{Er}_x\text{Y}_{2-x}\text{CaGe}_4\text{O}_{12}$ ,  $x=0.05\text{--}1.5$ . The numeration of the bands corresponds to transitions: (1)  ${}^2\text{H}_{11/2} \rightarrow {}^4\text{I}_{15/2}$  (526 nm); (2)  ${}^4\text{S}_{3/2} \rightarrow {}^4\text{I}_{15/2}$  (545 nm); (3)  ${}^4\text{F}_{9/2} \rightarrow {}^4\text{I}_{15/2}$  (670 nm). The inset plots show the concentration dependence for two green lines and their pump power dependence. The laser excitation wavelength is 808 nm.

Irrespective of the used laser excitation wavelengths  $\lambda_{\text{em}}=808$  nm and  $\lambda_{\text{em}}=980$  nm one can distinguish well-known green luminescence lines around 526 nm and 545 nm originated from the  $f\text{--}f$  transitions  ${}^2\text{H}_{11/2} \rightarrow {}^4\text{I}_{15/2}$  and  ${}^4\text{S}_{3/2} \rightarrow {}^4\text{I}_{15/2}$ . Nevertheless under 808 nm laser excitation no visible emission line  $\sim 670$  nm caused by the transition  ${}^4\text{F}_{9/2} \rightarrow {}^4\text{I}_{15/2}$  could be observed (Fig. 5). A number of efforts have been made to register any emission in the wavelength range 650–680 nm, series of spectral filters has been used but any distinguishable luminescent band has not been recorded. The red line at  $\sim 670$  nm could be assumed to be very weak. One makes an assumption of two different excitation routes for  ${}^2\text{H}_{11/2}$  and  ${}^4\text{S}_{3/2}$  multiplets. Note the highest emission signal in the wavelength range 525–545 nm has been revealed in the sample  $\text{Er}_{0.2}\text{Y}_{1.8}\text{CaGe}_4\text{O}_{12}$ . Taking into account the  ${}^4\text{I}_{9/2}$  level excitation in erbium ions, using an 808 nm diode laser, and the less active  $\text{Er}^{3+}$  centers in  $\text{Er}_{0.1}\text{Yb}_{0.1}\text{Y}_{1.8}\text{CaGe}_4\text{O}_{12}$  in comparison with  $\text{Er}_{0.2}\text{Y}_{1.8}\text{CaGe}_4\text{O}_{12}$ , the emission intensity of  $\text{Y}_2\text{CaGe}_4\text{O}_{12}:\text{Er}^{3+}$  is higher (additional Fig. 6). At the same time intensity values for the green line for  $\text{Er}_{0.1}\text{Yb}_{0.1}\text{Y}_{1.8}\text{CaGe}_4\text{O}_{12}$  correlate straight with concentration dependence for  $\text{Er}_x\text{Y}_{2-x}\text{CaGe}_4\text{O}_{12}$ , as it is shown in the left inset in Fig. 5.

Concerning the obtained results a schematic diagram of the energy level positions of the two trivalent lanthanide ions in  $\text{Y}_2\text{CaGe}_4\text{O}_{12}:\text{Er}^{3+}$  and  $\text{Y}_2\text{CaGe}_4\text{O}_{12}:\text{Er}^{3+}, \text{Yb}^{3+}$  has been proposed (Fig. 7). Some of the most important ground state (GSA) and

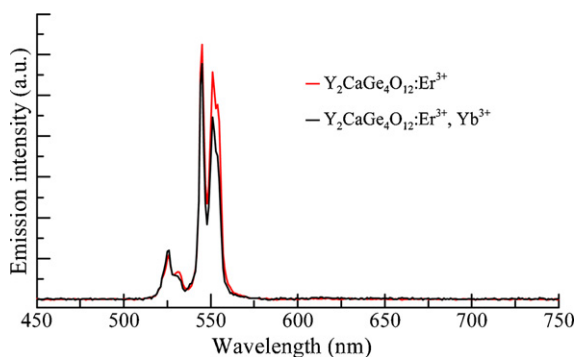


**Fig. 6.** Emission spectra of the optimized samples  $\text{Y}_2\text{CaGe}_4\text{O}_{12}:\text{Er}^{3+}$  and  $\text{Y}_2\text{CaGe}_4\text{O}_{12}:\text{Er}^{3+}, \text{Yb}^{3+}$ . The laser excitation wavelength is 808 nm.

excited state absorption (ESA), energy transfer upconversion (ETU) and nonradiative multiphonon relaxation processes occurring in erbium and ytterbium ions are also illustrated. Besides the visible emission transitions, rather strong infrared emissions exist [16], that is also indicated. Numerical energy values are given based on diffuse reflection spectral data and NIR absorption spectra, measured for the  $\text{Er}_2\text{CaGe}_4\text{O}_{12}$  and  $\text{Yb}_2\text{CaGe}_4\text{O}_{12}$  samples (Fig. 8a and b).

A laser pumping at wavelength  $\lambda_{\text{ex}}=980$  nm leads to cascade two-step (GSA and ESA) excitation of the  ${}^4\text{F}_{7/2}$  level (band in the wavelength range 473–504 nm). The following process of multiphonon relaxation populates the  ${}^2\text{H}_{11/2}$  and  ${}^4\text{S}_{3/2}$  states, initial for the green emission. Thus, under NIR irradiation the most intensive luminescence bands around 526 and 545 nm originate from  ${}^2\text{H}_{11/2}$  and  ${}^4\text{S}_{3/2}$  levels. Upon 980 nm excitation the possible ETU process would consist of a pair of energy conserving transitions ( ${}^4\text{I}_{11/2} \rightarrow {}^4\text{I}_{15/2}$ ,  ${}^4\text{I}_{11/2} \rightarrow {}^4\text{F}_{7/2}$ ) in  $\text{Y}_2\text{CaGe}_4\text{O}_{12}:\text{Er}^{3+}$ . The influence of the ETU process arises from ytterbium and erbium codoping of the  $\text{Y}_2\text{CaGe}_4\text{O}_{12}$  host compound. In certain case the  $\text{Yb}^{3+} {}^2\text{F}_{5/2}$  and  $\text{Er}^{3+} {}^4\text{I}_{11/2}$  states are at such energies that direct excitation into these states is possible, i.e. the application of the laser irradiation at 980 nm in present work. As there is a reasonable estimation that the majority of the excitation photons would be absorbed by  $\text{Yb}^{3+}$  (absorption cross-section is larger than at  $\text{Er}^{3+} {}^4\text{I}_{11/2}$  state) and ytterbium ions have no higher-lying excited states than the  ${}^2\text{F}_{5/2}$ , these ions would perform energy transfer upconversion with erbium species in order for visible emission intensification to occur. In the energy range illustrated in Fig. 7  $\text{Yb}^{3+}$  has some energy transfer possibilities to erbium ions; it is denoted with dotted arrows. There are three energy transfer paths  $\text{Yb}^{3+} \rightarrow \text{Er}^{3+}$  in  $\text{Y}_2\text{CaGe}_4\text{O}_{12}:\text{Er}^{3+}, \text{Yb}^{3+}$ , which induces the erbium transitions  ${}^4\text{I}_{15/2} \rightarrow {}^4\text{I}_{11/2}$ ,  ${}^4\text{I}_{11/2} \rightarrow {}^4\text{F}_{7/2}$  and  ${}^4\text{I}_{13/2} \rightarrow {}^4\text{F}_{9/2}$ . The third excitation route is due to inclusion of nonradiative multiphonon relaxation  ${}^4\text{I}_{11/2} \rightarrow {}^4\text{I}_{13/2}$ . Therefore, there are three different erbium levels ( ${}^2\text{H}_{11/2}$ ,  ${}^4\text{S}_{3/2}$  and  ${}^4\text{F}_{9/2}$ ) that are populated because of two-photon ETU process. Besides an intensive NIR emission  ${}^4\text{I}_{13/2} \rightarrow {}^4\text{I}_{15/2}$  reflects the population of the  ${}^4\text{I}_{13/2}$  state that makes an additional suggestion for the red emission to originate from the  ${}^4\text{I}_{13/2} \rightarrow {}^4\text{F}_{9/2}$  excitation transition. Making an assumption of ytterbium–erbium energy transfer and ESA for re-excitation of the  ${}^4\text{I}_{13/2}$  state, one should take into account an energy mismatch  $\sim 850\text{--}1400$   $\text{cm}^{-1}$ , the latter should be compen-

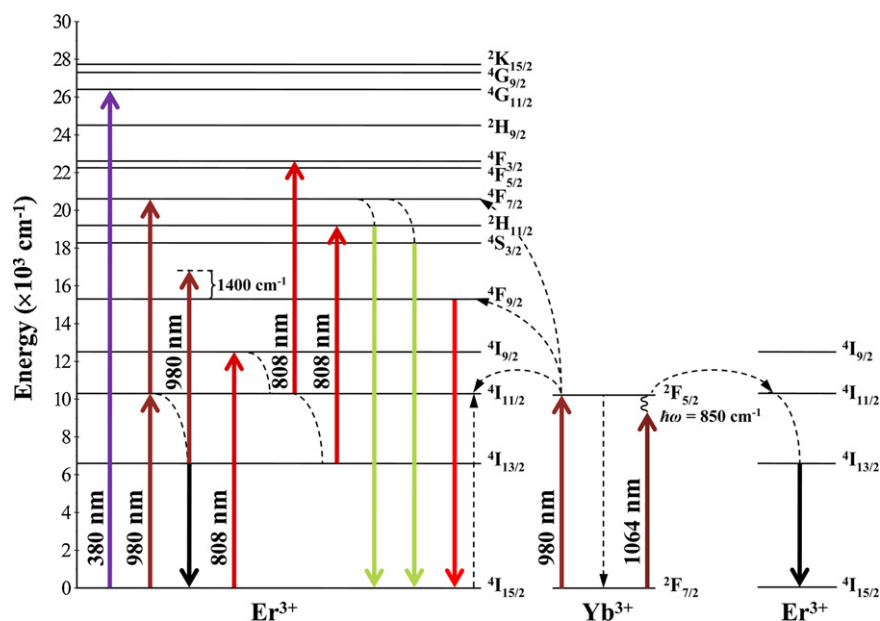


**Fig. 7.** Schematic energy level diagram, upconversion excitation, visible and infrared emission schemes for the erbium and ytterbium ions. Full and dotted arrows indicate radiative and nonradiative energy transfer processes, respectively. Dash lines denote nonradiative multiphonon relaxations.

sated by phonon assistance [31]. Fig. 8c shows the typical Raman spectrum of a  $\text{Ln}_2\text{CaGe}_4\text{O}_{12}$ ,  $\text{Ln} = \text{Y}, \text{Yb}$ , sample, obtained at room temperature using  $\text{Ar}^+$  laser irradiation,  $\lambda_{\text{ex}} = 514.5 \text{ nm}$ . The Raman scattering measurements for erbium doped specimens consistently reveal the photoluminescence obscuring the much weaker Raman signal even at the lowest doping contents of  $\text{Er}^{3+}$  ions. The dominant phonon modes are found to be at  $\sim 850 \text{ cm}^{-1}$  (O(2)–Ge–O(2) terminal bonds) and  $\sim 505 \text{ cm}^{-1}$  (Ge–O(1)–Ge bridge bonds), they are attributed to the totally symmetric vibrations. Therefore, the second upward excitation from  $^4\text{I}_{13/2}$  to  $^4\text{F}_{9/2}$  is possible with the assistance of 1–2 phonons of the germanate host.

### 3.2. Upconversion luminescence under 808 nm excitation

Incident laser irradiation at 808 nm supplies the excitation of the  $^4\text{I}_{9/2}$  level in  $\text{Er}^{3+}$  (GSA). There are several possible further excitation and emission mechanisms, involving a number of ETU, ESA, cross-relaxation and nonradiative multiphonon relaxation processes. The ESA process  $^4\text{I}_{9/2} \rightarrow ^2\text{H}_{9/2}$  is unlikely in  $\text{Y}_2\text{CaGe}_4\text{O}_{12}:\text{Er}^{3+}$ . The lifetime of the  $^4\text{I}_{9/2}$  level is known to be comparatively short in many erbium doped systems [32]. Besides in oxide host materials with

rather high phonon energies, the  $^4\text{I}_{9/2}$  lifetime is strongly quenched by multiphonon relaxation [33]. The second reason is in the estimation of multiphonon relaxation probability. The energy band  $^2\text{H}_{9/2}$  is in the  $\Delta E = 24,096\text{--}24,876 \text{ cm}^{-1}$  range. The minimal energy difference between  $^2\text{H}_{9/2}$  and  $^2\text{H}_{11/2}$  states is about  $4250 \text{ cm}^{-1}$ , according to the diffuse reflection spectra. This value is approximately equal to the highest phonon mode  $\sim 850 \text{ cm}^{-1}$  multiplied by five. The contribution of the possible multiphonon relaxation could be assessed based on the so-called “energy gap law” in the weak coupling limit that relates the rate of the relaxation to the number of the highest energy phonons available in the host matrix which are needed to bridge the energy interval between the luminescent level and the next lower energy level [34,35]:

$$k_{\text{nr}} \propto e^{-\beta g}, \quad (1)$$

implying the exponential decrease of the nonradiative rate constant  $k_{\text{nr}}$  with increasing energy gap. The specific constant  $\beta$  is a characteristic of the material, and  $g$  is the reduced energy gap in units of the maximal vibrational mode  $\hbar\omega_{\text{max}}$ . According to the known rule-of-thumb for an  $f$ -electron system the radiative relaxation is dominant when the reduced energy gap to the next

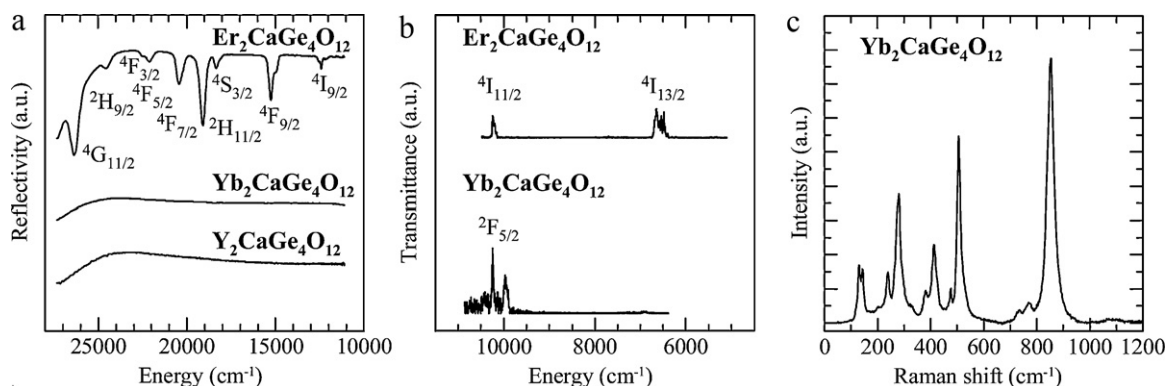


**Fig. 8.** Spectroscopic data for  $\text{Ln}_2\text{CaGe}_4\text{O}_{12}$ ,  $\text{Ln} = \text{Er}, \text{Yb}$ : diffuse reflection spectra of the samples measured at room temperature (a) and absorption spectra at  $T = -180^\circ\text{C}$  with denoted series of transitions in  $\text{Ln}^{3+}$  ions from their ground states to different excited states (b). Typical room temperature Raman spectrum of a tetrametagermanate  $\text{Ln}_2\text{CaGe}_4\text{O}_{12}$ ,  $\text{Ln} = \text{Yb}, \text{Y}$ ,  $\lambda_{\text{ex}} = 514.5 \text{ nm}$  (c).

lowest level is more than five high energy phonons, i.e.  $g > 5$ , while for smaller gaps nonradiative multiphonon emission becomes the major depopulation process [36–38]. There is a somewhat intermediate condition for the radiationless transition  ${}^2\text{H}_{9/2} \rightarrow {}^2\text{H}_{11/2}$  in  $\text{Y}_2\text{CaGe}_4\text{O}_{12}:\text{Er}^{3+}$ . On the other hand any detectable emission signal caused by the radiative relaxation from  ${}^2\text{H}_{9/2}$  to the lower or ground state has not been detected. Therefore, in erbium doped  $\text{Y}_2\text{CaGe}_4\text{O}_{12}$  the  ${}^2\text{H}_{11/2}$  and  ${}^4\text{S}_{3/2}$  excited states are not reached via the ESA process  ${}^4\text{I}_{9/2} \rightarrow {}^2\text{H}_{9/2}$  and the following nonradiative transitions.

When  ${}^4\text{I}_{9/2}$  level is excited, the population will relax quickly the  ${}^4\text{I}_{11/2}$  level, as well as the lower  ${}^4\text{I}_{13/2}$  level. For these states the excitation pathways to feed the  ${}^2\text{H}_{11/2}$  and  ${}^4\text{S}_{3/2}$  levels using an 808 nm irradiation would be considered. As this excitation implies the GSA process from  ${}^4\text{I}_{15/2}$  to  ${}^4\text{I}_{9/2}$  multiplet, the latter is separated from the next lower energy level  ${}^4\text{I}_{11/2}$  by approximately  $\Delta E = 2000 \text{ cm}^{-1}$ . The energy gap between  ${}^4\text{I}_{11/2}$  and  ${}^4\text{I}_{13/2}$  states is about  $3420 \text{ cm}^{-1}$ , that corresponds to four highest energy phonons. Two consequent nonradiative multiphonon relaxation processes  ${}^4\text{I}_{9/2} \rightarrow {}^4\text{I}_{11/2}$  and  ${}^4\text{I}_{11/2} \rightarrow {}^4\text{I}_{13/2}$  can be assumed, they are also revealed in many other erbium doped host matrices with maximal phonon energies around  $\sim 850 \text{ cm}^{-1}$ , a number of similar examples has been discussed elsewhere [39–44]. That is why for 808 nm excitation the following ESA steps  ${}^4\text{I}_{11/2} \rightarrow {}^4\text{F}_{3/2}$ ,  ${}^4\text{F}_{5/2}$  and  ${}^4\text{I}_{13/2} \rightarrow {}^2\text{H}_{11/2}$  may be possible to further green emissions due to  ${}^2\text{H}_{11/2} \rightarrow {}^4\text{I}_{15/2}$  and  ${}^4\text{S}_{3/2} \rightarrow {}^4\text{I}_{15/2}$  transitions. Nonradiative relaxation via  ${}^4\text{F}_{3/2}$ ,  ${}^4\text{F}_{5/2} \rightarrow {}^2\text{H}_{11/2}$  is likely to occur in this case ( $\Delta E \sim 2$  highest energy phonons). Note the listed energy evaluations based on the room temperature spectroscopic experiments. However the influence of nonradiative multiphonon relaxation mechanisms in this discussion is not straightforward in the absence of luminescence spectral data in NIR range obtained using an 808 nm laser excitation, as well as time-resolved upconversion emission measurements. This will be the subject of the future research. As visible emission line  $\sim 670 \text{ nm}$  caused by the transition  ${}^4\text{F}_{9/2} \rightarrow {}^4\text{I}_{15/2}$  has not been observed (Fig. 5), an assumption of very weak intensity of this line  $\sim 670 \text{ nm}$  has been proposed. In the case of the red emission the population of the level  ${}^4\text{F}_{9/2}$  at low erbium concentrations is usually due to multiphonon relaxation from the  ${}^4\text{S}_{3/2}$  level, the red emission is often rather weak in comparison with green one, the similar result has been revealed in erbium doped lead niobium germanate glasses with the maximum phonon energy of the lattice  $\sim 810 \text{ cm}^{-1}$  [41]. Another explanation may be given based on recent studies of  $\text{LaVO}_4:\text{Er}^{3+}$  crystal, which has revealed the intensive green and NIR luminescence [43], for this material possessing the dominant vibrational mode at  $912 \text{ cm}^{-1}$  a series of multiphonon relaxations has been considered. The simultaneous emission of three phonons is sufficient to transfer the  ${}^4\text{F}_{9/2}$  excitation to the next lower  ${}^4\text{I}_{9/2}$  level. Four phonons are created during multiphonon processes that contribute to the depletion of the  ${}^4\text{S}_{3/2}$  and  ${}^4\text{I}_{11/2}$  states. Taking into account the energy gap between the  ${}^4\text{F}_{9/2}$  and  ${}^4\text{I}_{9/2}$  levels is close to the value of the highest phonon energy multiplied by three in  $\text{Y}_2\text{CaGe}_4\text{O}_{12}:\text{Er}^{3+}$  the similar mechanism of multiphonon relaxation in the decay of intermediate states can be assumed upon an 808 nm laser excitation. A laser irradiation at  $\lambda_{\text{ex}} = 808 \text{ nm}$  may provide several ETU processes: ( ${}^4\text{I}_{9/2} \rightarrow {}^4\text{I}_{15/2}$ ,  ${}^4\text{I}_{9/2} \rightarrow {}^2\text{H}_{9/2}$ ), ( ${}^4\text{I}_{11/2} \rightarrow {}^4\text{I}_{15/2}$ ,  ${}^4\text{I}_{11/2} \rightarrow {}^4\text{F}_{7/2}$ ) and ( ${}^4\text{I}_{9/2} \rightarrow {}^4\text{I}_{15/2}$ ,  ${}^4\text{I}_{13/2} \rightarrow {}^2\text{H}_{11/2}$ ). But only the second ETU scheme probably occurs, as the population of the  ${}^4\text{I}_{9/2}$  level is usually very weak. Laser pumping at 808 nm resonantly to the  ${}^4\text{I}_{9/2}$  state of erbium without direct ytterbium excitation may also stimulate an emission in  $\text{Y}_2\text{CaGe}_4\text{O}_{12}:\text{Er}^{3+}, \text{Yb}^{3+}$  in the 960–1060 nm wavelength range that will correspond to ytterbium, because of possible back energy transfer  $\text{Er}^{3+} \rightarrow \text{Yb}^{3+}$  [45]. Nevertheless, the determination of the main ETU mechanism will be discussed elsewhere in future.

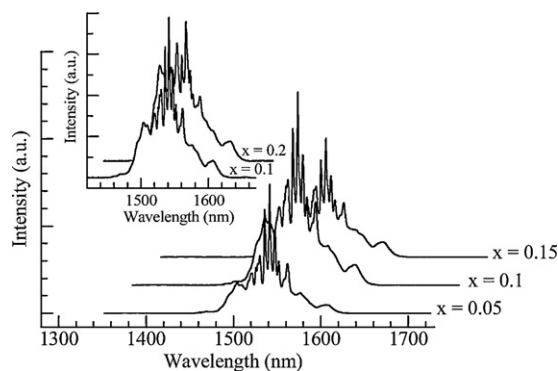
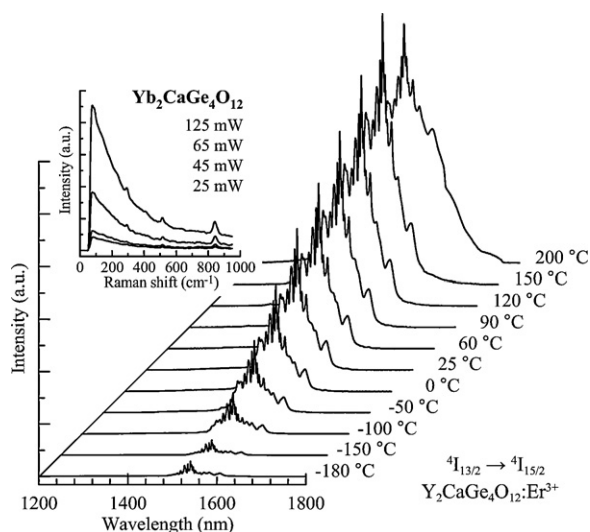


Fig. 9. Emission spectra of the samples  $\text{Er}_x\text{Yb}_{0.2-x}\text{Y}_{1.8}\text{CaGe}_4\text{O}_{12}$ ,  $x = 0.05\text{--}0.2$ . The laser excitation wavelength is 1064 nm; pump power is less than 100 mW.

### 3.3. NIR emission spectra under 1064 nm excitation

Besides 808 nm and 980 nm laser sources, NIR excitation with wavelength  $\lambda_{\text{ex}} = 1064 \text{ nm}$  has been used to study converted luminescence in  $\text{Y}_2\text{CaGe}_4\text{O}_{12}:\text{Er}^{3+}, \text{Yb}^{3+}$ . Visible emission owing to the cooperative energy transfer in the nonresonant system may occur via phonon-assisted process. The nonresonant energy transfer is associated with emission or absorption of phonons to balance the energy mismatch  $\Delta E$  according to the Miyakawa–Dexter theory [46,47]. In erbium doped  $\text{Y}_2\text{CaGe}_4\text{O}_{12}$  sensitized with trivalent ytterbium under quasi-resonance  $\lambda_{\text{ex}} = 1064 \text{ nm}$  excitation that is lower than the ytterbium  ${}^2\text{F}_{7/2} \rightarrow {}^2\text{F}_{5/2}$  transition, the excitation mechanism demands the participation of optical phonons in order to compensate for the energy mismatch of  $\sim 850 \text{ cm}^{-1}$  between the pump photon and the ytterbium excitation energy. It consequently depends on the phonon occupation number in the optical host material. Note the highest vibrational mode in the  $\text{Y}_2\text{CaGe}_4\text{O}_{12}$  host matrix is  $\sim 850 \text{ cm}^{-1}$ . The population of the rare-earth activator ion emitting levels is accomplished by means of multiphonon-assisted anti-Stokes sideband excitation of the sensitizer ions, followed by successive energy transfer processes to the active emitter [17,18]. There are two main competing processes that depend on temperature increase in this case, i.e. multiphonon relaxation and anti-Stokes phonon-assisted upconversion excitation. However for various rare-earth doped systems (chalcogenide, tellurite glasses, glass ceramics, optical fibers, etc.) thermal intensity enhancement of multiphonon-assisted anti-Stokes upconversion emission has been shown up to the temperature values around  $200^\circ\text{C}$  [18,48–52]. The above listed examples for visible emission occurrence have been obtained using high power laser sources ( $P_{\text{pump}} > 700 \text{ mW}$ ,  $\lambda_{\text{ex}} = 1064 \text{ nm}$ ) and beam focusing for achieving the higher power density. For  $\text{Y}_2\text{CaGe}_4\text{O}_{12}:\text{Er}^{3+}, \text{Yb}^{3+}$  laser pumping with excitation wavelength  $\lambda_{\text{ex}} = 1064 \text{ nm}$  has been used in the low-power regime. The  $\text{Y}_2\text{CaGe}_4\text{O}_{12}:\text{Er}^{3+}, \text{Yb}^{3+}$  samples have not revealed visible upconversion emission for pump power values less than 100 mW. Emissions have been detected in the NIR range owing to the  $f\text{--}f$  transition  ${}^4\text{I}_{13/2} \rightarrow {}^4\text{I}_{15/2}$  in erbium ions (Fig. 9). Ytterbium sensitizing leads to very moderate rise of the intensity, however the  $\text{Er}_{0.1}\text{Yb}_{0.1}\text{Y}_{1.8}\text{CaGe}_4\text{O}_{12}$  sample has the highest emission signal. It can be account for small efficiency of this process, which implies phonon-assisted anti-Stokes sideband excitation of the  $\text{Yb}^{3+}$  ions and quasi-resonant energy transfer  $\text{Yb}^{3+} \rightarrow \text{Er}^{3+}$ , the following decay via nonradiative multiphonon relaxation  ${}^4\text{I}_{11/2} \rightarrow {}^4\text{I}_{13/2}$  and emission causing from  ${}^4\text{I}_{13/2} \rightarrow {}^4\text{I}_{15/2}$ . The results of preliminary experiments on erbium doped  $\text{Y}_2\text{CaGe}_4\text{O}_{12}$  prove the possibility of the above mentioned processes. Fig. 10 shows temperature dependence for this luminescence band ( $-180^\circ\text{C} < T < 200^\circ\text{C}$ ). NIR emission enhancement under quasi-resonance excitation occurs with the temperature increase.



**Fig. 10.** Thermal increase of the NIR emission intensity in the spectra of  $\text{Y}_2\text{CaGe}_4\text{O}_{12}:\text{Er}^{3+}$  ( $-180^\circ\text{C} < T < 200^\circ\text{C}$ ). The laser excitation wavelength is 1064 nm. The inset plot shows the Raman spectrum of the  $\text{Yb}_2\text{CaGe}_4\text{O}_{12}$  sample.

Low efficiency of the ascribed processes in erbium–ytterbium codoped tetrametagermanate can be also realized taking into account the Raman spectrum of  $\text{Yb}_2\text{CaGe}_4\text{O}_{12}$ , obtained under 1064 nm excitation. Raman effect is known to be less efficient and intensive than luminescence caused by  $f$ – $f$  radiative transitions, and the latter usually suppresses Stokes and anti-Stokes Raman lines in the spectrum. Still in addition to Raman scattering peaks a luminescent tail around  $\Delta\nu = 0 \text{ cm}^{-1}$  is found in ytterbium doped  $\text{Y}_2\text{CaGe}_4\text{O}_{12}$ , that originates from the radiative transition  $^4\text{F}_{5/2} \rightarrow ^4\text{F}_{7/2}$  in  $\text{Yb}^{3+}$  ions (inset in Fig. 10), although an influence of concentration quenching takes place in  $\text{Yb}_2\text{CaGe}_4\text{O}_{12}$ . Therefore, NIR emission under quasi-resonance excitation is comparatively weak for pump power values less than 100 mW.

#### 4. Conclusions

Upconversion emission in visible spectral range under NIR excitation,  $\lambda_{\text{ex}} = 980 \text{ nm}$  has been found in the calcium yttrium tetrametagermanates  $\text{Y}_2\text{CaGe}_4\text{O}_{12}$  doped with  $\text{Er}^{3+}$  and  $\text{Er}^{3+}/\text{Yb}^{3+}$ . The luminescence was intense enough to be seen by naked eye. The power dependence of the visible luminescence lines measured at room temperature in the low-power limit indicated the two-photon upconversion process. In the  $\text{Y}_2\text{CaGe}_4\text{O}_{12}:\text{Er}^{3+}$ ,  $\text{Yb}^{3+}$  samples green and red emissions increased several times more owing to energy transfer  $\text{Yb}^{3+} \rightarrow \text{Er}^{3+}$ . The other upconversion excitation mechanism in  $\text{Y}_2\text{CaGe}_4\text{O}_{12}:\text{Er}^{3+}$  has been shown for 808 nm incident laser irradiation. A scheme of excitation and emission routes involved ground/excited state absorption, energy transfer upconversion, nonradiative multiphonon relaxation processes in trivalent lanthanide ions in  $\text{Y}_2\text{CaGe}_4\text{O}_{12}:\text{Er}^{3+}$  and  $\text{Y}_2\text{CaGe}_4\text{O}_{12}:\text{Er}^{3+}$ ,  $\text{Yb}^{3+}$  has been proposed. There was only NIR luminescence found in erbium doped  $\text{Y}_2\text{CaGe}_4\text{O}_{12}$  sensitized with trivalent ytterbium under quasi-resonance  $\lambda_{\text{ex}} = 1064 \text{ nm}$  excitation that was lower than the ytterbium  $^2\text{F}_{7/2} \rightarrow ^2\text{F}_{5/2}$  transition. Conditions for visible emission depending on pump power have been briefly considered. Only NIR emission caused by the  $^4\text{I}_{13/2} \rightarrow ^4\text{I}_{15/2}$  transition in erbium ions has been detected in the low-power regime ( $P_{\text{pump}} \leq 100 \text{ mW}$ ). Further detailed study of upconversion luminescence concentration dependence on the erbium–ytterbium codoping, as well as the determination of the main ETU mechanisms based on time-resolved luminescence spectroscopy would be discussed elsewhere.

#### Acknowledgements

This work was supported by the RFBR under grant No. 10-03-96028 r\_ural\_a, and grants sponsored by UB RAS (grant Nos. 09-P-3-1009 and 10-3-02). The authors are grateful to A.I. Kuznetsova (DCGE, CICECO, UA, Aveiro, Portugal) and S.R. Nabiev (IIP UB RAS, Ekaterinburg, Russia) for their assistance.

#### References

- [1] T. Sandrock, H. Scheife, E. Heumann, G. Huber, *Opt. Lett.* 22 (1997) 808.
- [2] E. Downing, L. Hesselink, J. Ralston, R. Macfarlane, *Science* 273 (1996) 1185.
- [3] S.Q. Xu, H.P. Ma, D.W. Fang, Z.X. Zhang, Z.H. Jiang, *Mater. Lett.* 59 (2005) 3066.
- [4] C.G. Morgan, S. Dad, A.C. Mitchell, *J. Alloys Compd.* 451 (2008) 526.
- [5] Y. Saito, M. Kato, A. Nomura, T. Kano, *Appl. Phys. Lett.* 56 (1990) 811.
- [6] C. Ronda, *Luminescence: From Theory to Application*, WILEY VCH Verlag GmbH & Co. KGaA, Weinheim, 2008.
- [7] F. Auzel, *Chem. Rev.* 104 (2004) 139.
- [8] U. Hömmerich, E.E. Nyein, S.B. Trivedi, *J. Lumin.* 113 (2005) 100.
- [9] A.M. Tkachuk, S.E. Ivanova, M.-F. Joubert, Y. Guyot, L.I. Isaenko, V.P. Gapontsev, *J. Lumin.* 125 (2007) 271.
- [10] J. Méndez-Ramos, V.K. Tikhomirov, V.D. Rodríguez, D. Furniss, *J. Alloys Compd.* 440 (2007) 328.
- [11] K. Horchani, J.C. Gâcon, C. Dujardin, N. Garnier, C. Garapon, M. Férid, M. Trabelsi-Ayedi, *J. Lumin.* 94–95 (2001) 69.
- [12] K. Horchani, J.C. Gâcon, C. Dujardin, N. Garnier, M. Férid, M. Trabelsi-Ayedi, *Nucl. Instrum. Methods Phys. Res. A* 486 (2002) 283.
- [13] H. Jacobsen, G. Meyer, W. Schipper, G. Blasse, *Z. Anorg. Allg. Chem.* 620 (1994) 451.
- [14] V.G. Zubkov, L.L. Surat, A.P. Tyutyunnik, I.F. Berger, N.V. Tarakina, B.V. Slobodin, M.V. Kuznetsov, T.A. Denisova, N.A. Zhuravlev, L.A. Perelyaeva, I.V. Baklanova, I.R. Shein, A.L. Ivanovskii, B.V. Shulgin, A.V. Ishchenko, A.N. Tcherepanov, G. Svensson, B. Forslund, M.Yu. Skripkin, *Phys. Rev. B* 77 (2008) 174113.
- [15] N.V. Tarakina, V.G. Zubkov, I.I. Leonidov, A.P. Tyutyunnik, L.L. Surat, J. Hadermann, G. Van Tendeloo, *Z. Kristallogr.* 30 (2009) 401 (Supplement).
- [16] V.G. Zubkov, I.I. Leonidov, A.P. Tyutyunnik, N.V. Tarakina, L.L. Surat, L.A. Perelyaeva, I.V. Baklanova, O.V. Koryakova, *J. Lumin.* 129 (2009) 1625.
- [17] F. Auzel, *Phys. Rev. B* 13 (1976) 2809.
- [18] A.S. Gouveia-Neto, L.A. Bueno, R.F. Nascimento, E.A. Silva, E.B. da Costa, *Mater. Lett.* 63 (2009) 1999.
- [19] J.A. Campá, C. Cascales, E. Gutiérrez-Puebla, M.A. Monge, I. Rasines, C. Ruíz Valero, *J. Solid State Chem.* 124 (1996) 17.
- [20] H. Yamane, R. Tanimura, T. Yamada, J. Takahashi, T. Kajiwara, M. Shimada, *J. Solid State Chem.* 179 (2006) 289.
- [21] C. Taviot-Guého, P. Léone, P. Palvadeau, J. Rouxel, *J. Solid State Chem.* 143 (1999) 145.
- [22] V.G. Zubkov, N.V. Tarakina, I.I. Leonidov, A.P. Tyutyunnik, L.L. Surat, M.A. Melkozerova, E.V. Zabolotskaya, D.G. Kellerman, *J. Solid State Chem.* 183 (2010) 1186.
- [23] U. Lambert, W. Eysel, *Powder Diffr.* 1 (1986) 256.
- [24] C. Cascales, M.T. Fernandez Diaz, M.A. Monge, *Chem. Mater.* 12 (2000) 3369.
- [25] C. Cascales, M.A. Monge, *J. Alloys Compd.* 344 (2002) 379.
- [26] E.J. Baran, C.C. Wagner, A.E. Lavat, C. Cascales, *J. Raman Spectrosc.* 28 (1997) 927.
- [27] M. Pollnau, D.R. Gamelin, S.R. Lüthi, M.P. Hehlen, H.U. Güdel, *Phys. Rev. B* 61 (2000) 3337.
- [28] J.F. Suyver, A. Aebischer, S. García-Revilla, P. Gerner, H.U. Güdel, *Phys. Rev. B* 71 (2005) 125123.
- [29] V.V. Ovsyankin, P.P. Feofilov, *JETP Lett.* 3 (1966) 322.
- [30] F. Auzel, *F.C.R. Acad. Sci. (Paris)* 262 (1966) 1016.
- [31] H. Naruke, T. Mori, T. Yamase, *Opt. Mater.* 31 (2009) 1483.
- [32] D.Y. Wang, M. Yin, S.D. Xia, V.N. Makhov, N.M. Khaidukov, J.C. Krupa, *J. Alloys Compd.* 368 (2004) 337.
- [33] C. Ronda, *J. Lumin.* 129 (2009) 1824.
- [34] J.M.F. Van Dijk, M.F.H. Schuurmans, *J. Chem. Phys.* 78 (9) (1983) 5317.
- [35] G. Blasse, B.C. Grabmeier, *Luminescent Materials*, Springer-Verlag, Berlin, 1994.
- [36] T. Riedener, K.W. Krämer, H.U. Güdel, *Inorg. Chem.* 34 (1995) 2745.
- [37] D.R. Gamelin, H.U. Güdel, *Top. Curr. Chem.* 214 (2001) 1.
- [38] J.F. Suyver, A. Aebischer, D. Biner, P. Gerner, J. Grimm, S. Heer, K. Krämer, C. Reinhard, H.U. Güdel, *Opt. Mater.* 27 (2005) 1111.
- [39] M.B. Lee, J.H. Lee, B.G. Frederick, N.V. Richardson, *Surf. Sci.* 448 (2000) L207.
- [40] S.D. Cheng, C.H. Kam, Y. Zhou, Y.L. Lam, Y.C. Chan, S. Buddhudu, *Mater. Lett.* 45 (2000) 19.
- [41] R. Balda, A. Oleaga, J. Fernández, J.M. Fdez-Navarro, *Opt. Mater.* 24 (2003) 83.
- [42] X. Shen, Q.H. Nie, T.F. Xu, T. Peng, Y. Gao, *Phys. Lett. A* 332 (2004) 101.
- [43] R. Lisiecki, W. Ryba-Romanowski, E. Cavalli, M. Bettinelli, *J. Lumin.* 130 (2010) 131.
- [44] Z.S. Xiao, B. Zhou, L. Yan, F. Zhu, F. Zhang, A.P. Huang, *Phys. Lett. A* 374 (2010) 1297.
- [45] X. Mateos, R. Solé, Jna. Gavalda, M. Aguiló, F. Díaz, J. Massons, *J. Lumin.* 115 (2005) 131.

- [46] T. Miyakawa, D.L. Dexter, *Phys. Rev. B* 1 (1970) 2961.
- [47] W. Stręk, *Phys. Rev. B* 29 (1984) 6957.
- [48] P.V. dos Santos, E.A. Gouveia, M.T. de Araujo, A.S. Gouveia-Neto, A.S.B. Sombra, J.A. Medeiros Neto, *Appl. Phys. Lett.* 74 (1999) 3607.
- [49] C.J. da Silva, M.T. de Araujo, E.A. Gouveia, A.S. Gouveia-Neto, *Appl. Phys. B* 70 (2000) 185.
- [50] S.F. Felix, E.A. Gouveia, M.T. de Araujo, A.S.B. Sombra, A.S. Gouveia-Neto, *J. Lumin.* 87–89 (2000) 1020.
- [51] M.V.D. Vermelho, M.T. de Araujo, E.A. Gouveia, A.S. Gouveia-Neto, J.S. Aitchison, *Opt. Mater.* 17 (2001) 419.
- [52] P.V. dos Santos, M.V.D. Vermelho, E.A. Gouveia, M.T. de Araujo, A.S. Gouveia-Neto, F.C. Cassanjes, S.J.L. Ribeiro, Y. Messaddeq, *J. Alloys Compd.* 344 (2002) 304.